American Mineralogist, Volume 96, pages 250–260, 2011

Application of the two-feldspar geothermometer to ultrahigh-temperature (UHT) rocks in the Khondalite belt, North China craton and its implications

SHUJUAN JIAO* AND JINGHUI GUO

State Key Laboratory of Lithospheric Evolution, Institute of Geology and Geophysics, Chinese Academy of Sciences, Beijng 100029, China

ABSTRACT

The Paleoproterozoic Khondalite belt in the North China craton preserves evidence for ultrahigh-temperature (UHT) crustal metamorphism associated with the collision of the Yinshan and Ordos Blocks. Here we apply two-feldspar geothermometry to UHT granulites from two localities newly reported in this study (Tuguishan and Xuwujia) and another two localities from previous studies (Dajing/Tuguiwula and Dongpo) in the Khondalite belt. The presence of abundant perthite/mesoperthite in these rocks reflects post-peak slow cooling. The minimum estimated peak metamorphic temperatures are 832–998, 819–952, 844–1037, and 966–1019 °C computed at 8 kbar for the Dajing/Tuguiwula, Dongpo, Tuguishan, and Xuwujia areas, respectively. These results confirm the previous report of extreme metamorphism at Dajing/Tuguiwula and Dongpo, and reveal similar conditions in the new localities reported here, suggesting that UHT metamorphism is widespread in the Khondalite belt of the North China craton. Our study demonstrates that UHT metamorphism can be recognized using the two-feldspar geothermometry in rocks that do not possess other key UHT assemblages.

Keywords: Ultrahigh-temperature (UHT) metamorphism, two-feldspar geothermometer, perthite/mesoperthite, Paleoproterozoic, Khondalite belt, North China craton

INTRODUCTION

Ultrahigh-temperature (UHT) metamorphism takes place in the deep crust at extreme temperature conditions of 900–1100 °C and medium pressures (7–13 kbar; Harley 1998). Understanding the conditions and processes of UHT metamorphism provides important constraints on the nature of coupling between the crust, sub-crustal lithosphere, and asthenospheric mantle, as well as the tectonic setting of regional metamorphic belts (Lund et al. 2006; Harley 1998, 2004, 2008; Kelsey 2008; Santosh and Kusky 2010). The UHT diagnostic minerals and assemblages, such as Spr+Qz, Opx+Sil±Qz, or osumilite commonly occur in Mg-Al-rich rocks, and are rather scarce (Harley 1998, 2004, 2008). Since many of these minerals undergo retrogression, their original compositions are not often preserved, thereby narrowing the chance of direct evidence from diagnostic mineral assemblages. In this context, ternary feldspars (perthite, Per) provide a robust alternative, as they are more common than the diagnostic UHT assemblages and can be fairly resistant to retrograde resetting, making them useful for recognizing UHT metamorphism.

Recent studies in the Paleoproterozoic Khondalite belt of the North China craton have led to the discovery of UHT granulites, particularly from two localities at Dongpo and Dajing/Tuguiwula (Figs. 1 and 2) (Jin 1989; Liu et al. 2000; Guo et al. 2006, 2008; Santosh et al. 2006, 2007a, 2007b, 2009a; Liu et al. 2010). The UHT granulites at Dongpo are garnet-bearing and contain up to 30% sapphirine, as well as sillimanite, spinel, biotite, plagioclase, and minor cordierite, rutile, and ilmenite, but without quartz and orthopyroxene. Estimated peak UHT conditions are 910–980 °C and 8 kbar followed by a post-peak decompression (Fig. 2a) (Guo et al. 2006, 2008). In contrast, the UHT granulites at Dajing/Tuguiwula are Mg-Al-rich and contain the diagnostic UHT mineral assemblages of Spr+Qz, Al-rich Opx+Sil+Qz as well as ternary feldspar. Santosh et al. (2007a, 2009a) defined an anticlockwise *P-T* path with a peak metamorphic temperature of >970 °C at ~7–l3 kbar (Fig. 2b).

It is difficult to evaluate the extent of UHT metamorphism in this region because apart from the two UHT localities discussed above, rocks with diagnostic UHT mineral assemblages have not been recognized throughout the Khondalite belt. However, feldspars, which are appropriate for the application of two-feldspar geothermometry are commonly present in the granulite-facies rocks of this region and could provide an ideal means for evaluating the regional extent of UHT metamorphism in the Khondalite belt. Application of the modified two-feldspar geothermometer (Raase 1998; Hokada 2001; Hokada and Suzuki 2006; Prakash et al. 2006; Pilugin et al. 2009) has successfully defined the peak temperature conditions of HT/UHT metamorphism worldwide, primarily using the thermometer of Fuhrman and Lindsley (1988).

In this paper, we report the application of the modified two-feldspar geothermometer to granulite-facies rocks from two known UHT localities (Dongpo and Dajing/Tuguiwula) and two other localities in adjacent areas (Tuguishan and Xuwujia). Based on the results, we discuss the implications on regional UHT metamorphism in the Khondalite belt of the North China craton.

GEOLOGICAL SETTING

The North China craton is considered to have formed during collision between the Eastern and Western blocks along the Trans-North China orogen at ~1.85 Ga (Zhao et al. 2002, 2008a,

* Present address: No.19, Beitucheng West Road, Chaoyang, Beijing 100029, China. E-mail: jiaoshujuan0215@126.com

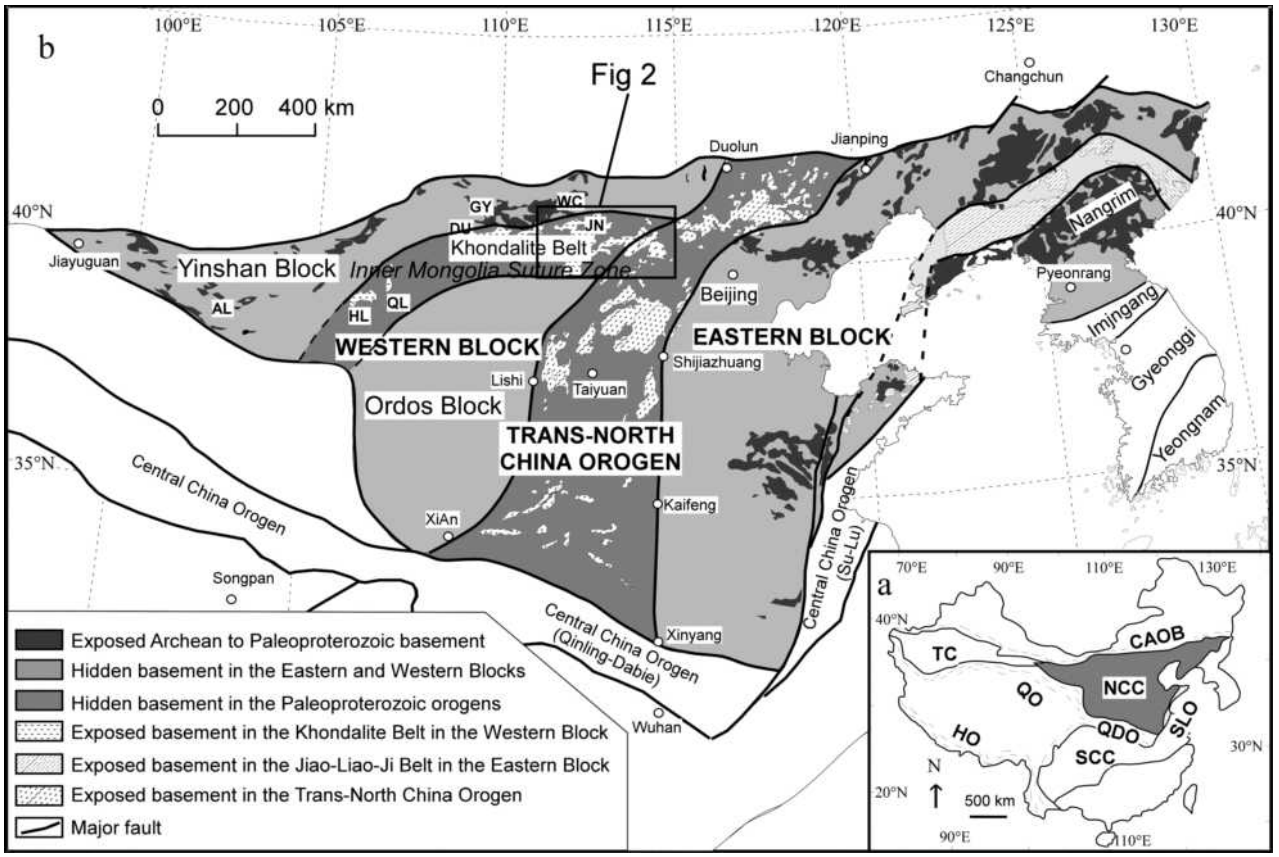

Figure 1. (**a**) Tectonic map of China showing the major cratons and young orogens [after Zhao et al. (2001)]. Area abbreviations: CAOB = Central Asian Orogenic belt; TC = Tarim craton; NCC = North China craton; QO = Qilianshan orogen; QDO = Qinling-Dabie orogen; SLO = Su-Lu orogen; HO = Himalaya orogen; SCC = South China craton. (**b**) Geological and tectonic map of the North China craton (after Zhao et al. 2005). Metamorphic complex abbreviations: AL = Alashan; DU = Daqingshan-Ulashan; HL = Helanshan; GY = Guyang; JN = Jining; QL = Qianlishan; WC = Wuchuan.

2008b; Guo et al. 2005; Kröner et al. 2006). The Western block formed by amalgamation of the Ordos block in the south and the Yinshan block in the north along the Khondalite belt at ~1.95 Ga (Zhao et al. 2005; Santosh et al. 2007b, 2009b; Yin et al. 2009) (Fig. 1). The collision zone between the Yinshan and Ordos blocks has been recently analyzed based on a detailed synthesis of geological, geophysical and tectonic information by Santosh (2010) and Santosh et al. (2010). These studies suggested that the zone defined a major collisional suture that preserved a record of Paleoproterozoic subduction-accretion collision tectonics associated with the collisional assembly of North China craton within the Columbia supercontinent (Rogers and Santosh, 2002, 2009). Santosh (2010) and Santosh et al. (2010) designated this zone as the Inner Mongolia Suture Zone.

The Khondalite belt is divisible into three terranes from west to east: Helanshan-Qianlishan (HL-QL), Daqingshan-Ulashan (DU), and Jining (JN) (Fig. 1b). The belt is mainly composed of granulite-facies metasedimentary rocks characterized by Grt+Crd+Sil+Gr (Lu et al. 1992, 1996; Zhao et al. 1999, 2005). The predominant rocks are quartzo-feldspathic gneiss, garnet- and sillimanite-bearing plagioclase gneiss, feldspathic quartzite, marble, and calc-silicate rocks. Additionally, in the Jining terrane (Fig. 2a) there are several syn- to post-tectonic garnet-bearing granites and minor charnockites derived from crustal melting (Guo et al. 1999; Zhai et al. 2003; Zhong et al. 2007). Many gabbroic, and noritic to dioritic intrusive bodies and their sedimentary host rocks in the Jining terrane are metamorphosed to granulite-facies conditions (Guo et al. 2001; Peng et al. in press).

Detrital zircon from sedimentary rocks in the Khondalite belt obtained ages in the range of ~2.0–1.96 Ga (Guo et al. 2001; Wu et al. 1998; Wan et al. 2006; Xia et al. 2006, 2008). Precise U-Pb dating of the UHT metamorphism revealed ages in the range of ~1.95–1.92 Ga (Santosh et al. 2007b, 2009b; Yin et al. 2009).

Outcrop geology and sample descriptions

The known UHT localities of Dongpo and Dajing/Tuguiwula in the Khondalite belt of the North China craton are situated in the eastern Daqingshan-Ulashan and central Jining terranes, respectively (Fig. 2). We collected samples from the sapphirine-bearing granulites, 1 km east of Dongpo village (locality 1 in Fig. 2a), and from the Dajing/Tuguiwula granulites in Dajing village (locality 3 in Fig. 2b). In addition, we also collected samples from two nearby localities where granulite-facies rocks without any diagnostic UHT assemblages: (1) Tuguishan (Tugui hill), 4 km west of Dajing village (locality 2 in Fig. 2b); (2) Xuwujia, 5 km south of Dajing village (locality 4 in Fig. 2b).

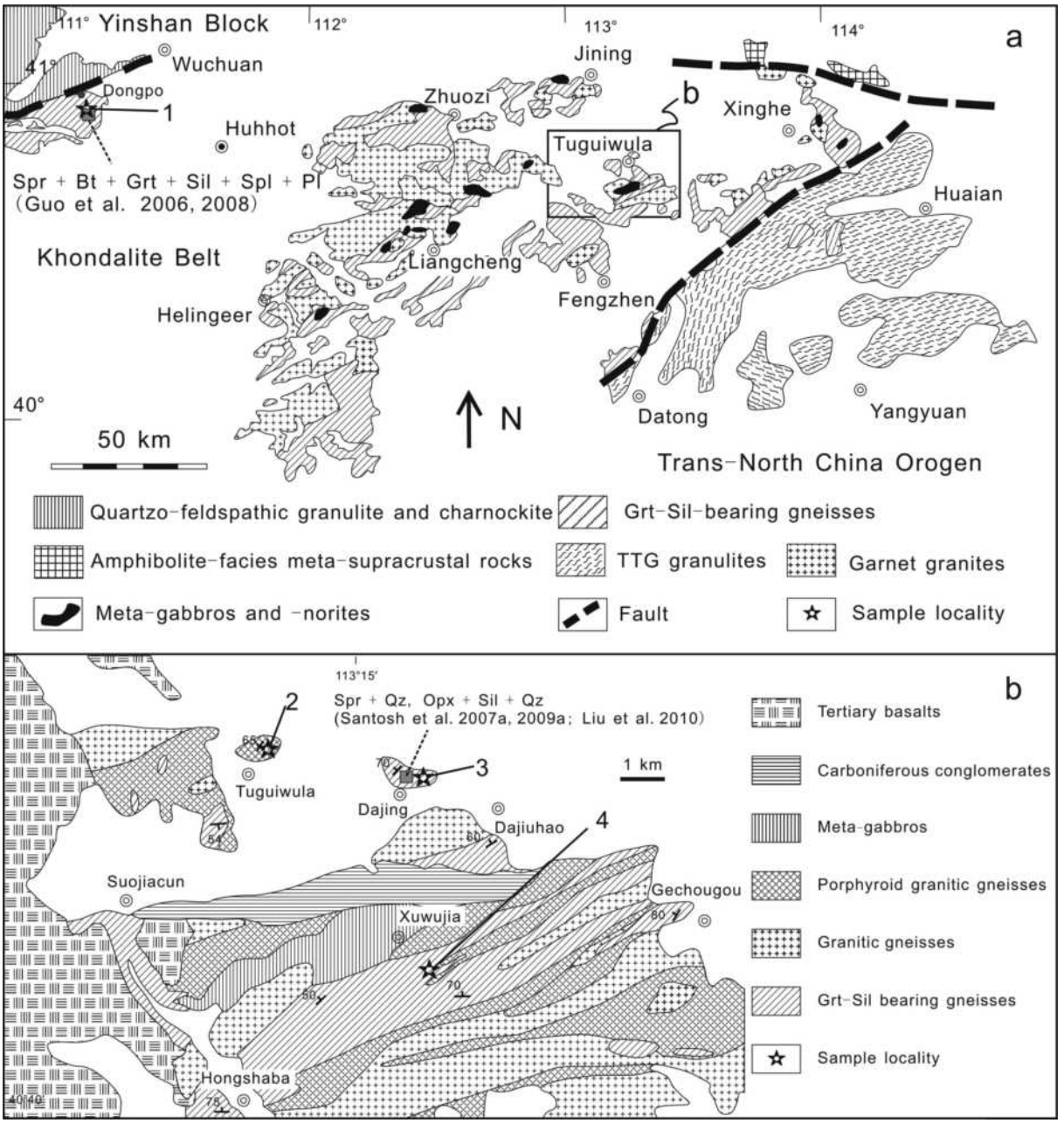

FIGURE 2. (**a**) Distribution of high-grade metamorphic rocks in the eastern segment of the Khondalite belt, North China craton [modified after Guo et al. (2001)]. (**b**) Simplified geological map of the Dajing /Tuguiwula area [modified after Liu et al. (2010)]. Sample localities: (1) The Dongpo outcrop; (2) the Tuguishan outcrop; (3) the Dajing/Tuguiwula outcrop; (4) the Xuwujia outcrop.

Samples from the Dajing/Tuguiwula outcrop

Eight samples are from the Dajing/Tuguiwula outcrop (locality 3 in Fig. 2b), ~5 km east of Tuguiwula town. This is the locality where the typical UHT granulites were discovered and described by Santosh et al. (2006, 2007a, 2007b, 2009a, 2009b) and Liu et al. (2010). The dominant UHT pelitic granulites have a strong foliation and are mutually intercalated with garnet-bearing felsic gneisses and garnet-bearing granites in this outcrop. Most of the pelitic granulites contain sapphirine, are enriched in Mg-Al, and have a banded structure composed of Grt+Sil+Spl-enriched melanosomes and quartzo-feldspathic leucosomes. The Grt-Sil-Spr granulites have 10–15% perthite and 5–10% plagioclase; all minerals are listed in Table 1. Plagioclase lamellae in perthite have a volume percentage of 8–26% (Fig. 3e). Garnet porphyroblasts generally contain mineral inclusions and even fascicular sillimanite grains (sample 08dj05). The sapphirine usually occurs as inclusion in garnet and sillimanite (Fig. 3a), or in the matrix surrounded by plagioclase (Fig. 3b). Radial Opx-Crd intergrowths are well developed around garnet.

Samples from the Dongpo outcrop

The Dongpo outcrop (locality 1 in Fig. 2a) hosts the main UHT garnetiferous sapphirine-bearing granulites described by

TABLE 1. Summary of the lithology and mineral assemblages of the analyzed samples

Locality	Lithology	Sample	Grt	Sil	Bt	Crd	Spr	Opx	Spl	Pl	Per/Mper	Rt	Qz	Ilm/Mag
Tuguishan	Grt-Sil granulite	07tgs01,05,08a1,09,11,12,18,19	+++	++	+	+	–	–	+	+	++	+	++	+
Dajing/Tuguiwula	Grt-Sil-Spr granulite	08dj03,05,09,11,12a,12b,13	+++	++	+	+	+	+	+	+	++	–	++	+
Xuwujia	Grt-Sil-Bt-Pl granulite	08xwj01a,03,04a,04b	+++	++	++	+	–	–	+	+	++	–	++	+
Dongpo	Spl-Grt-Bt-Pl granulite	04dq1-3	+++	–	+++	–	–	–	++	+++	+	–	–	+
Dongpo	Quartzo-feldspathic-Grt granulite	06dp20	++	–	+	–	–	–	–	++	+++	–	+++	+
Dongpo	Quartzo-feldspathic granulite	05dp02,04	+	–	++	–	–	–	–	++	+++	–	+++	+

Note: – = Not present; + = <10 vol%; ++ = 10–20 vol%; +++ = 20–50 vol%.

Guo et al. (2006, 2008). We have collected 4 samples from the rocks that surround and host these granulites. Sample 04dq1-3 is a Spl-Grt-Bt-Pl granulite that contains minor perthite (<5%) in the matrix and as inclusions in garnet porphyroblasts. Lamellae comprise only ~5% of perthite volume. Sample 06dp20 is a garnet-bearing, quartzo-feldspathic granulite that contains 25–30% perthite with ~10% lamellae. Fine-scale sub-lamellae occur among the main coarser lamellae (Fig. 3h). Samples 05dp02 and 05dp04 are both garnet-free, quartzo-feldspathic granulites. Sample 05dp02 has abundant mesoperthite (Mper), most of which contains up to 40% lamellae (Fig. 3g). Other included phases in the collected samples are listed in Table 1.

Samples from the Tuguishan outcrop

Eight pelitic granulite samples are from the Tuguishan outcrop, a small hill next to Tuguiwula town (locality 2 in Fig. 2b). All of the rocks are slightly foliated, and some show separation of Grt+Sil+Spl-enriched melanosome and quartzo-feldspathic leucosome, reflecting partial melting of the metasedimentary rocks. In addition, these pelitic granulites are associated with metagabbros, metanorites, charnockites, and garnet-bearing granites (Guo et al. in preparation). The Grt-Sil granulites contain 15–20% perthite and 5–10% plagioclase, in addition to other minerals listed in Table 1. Perthite lamellae are ordered and parallel (e.g., string, regular lamellar, rod textures, Fig. 3), and their volume percentages range from 5 to 27%.

Samples from the Xuwujia outcrop

Four samples, from Xuwujia village (locality 4 in Fig. 2b), ~5 km south of Dajing village, are close to the southern margin of a 1.92 Ga Xuwujia metagabbroic body (Fig. 2b). In this outcrop, pelitic Grt-Sil granulites and quartzo-feldspathic granulites are predominant, and they are highly deformed, sheared, and foliated. All samples are Grt-Sil-Bt-Pl granulites containing 15–20% perthite and <10% plagioclase; other minerals are listed in Table 1. Garnet porphyroblasts contain various mineral inclusions such as biotite, sillimanite, quartz, zircon, and ilmenite. Perthite lamellae are ordered with a volume percentage of >20% (Figs. 3d and 3f). Mesoperthite grains (i.e., the volume percentage of the lamellae is ~50%) are also present.

ANALYTICAL METHODS

Analytical procedures

Perthite/mesoperthite (lamella and host) grains and associated plagioclase grains were analyzed by electron microprobe (EMP) (Cameca SX51 and JEOL JXA-8100) at the Institute of Geology and Geophysics, Chinese Academy of Sciences in Beijing, China. Operating conditions were 15 kV and 10 nA with a 3 μm beam size. Count times were 20 s on peaks, and 10 s on each background, and natural and synthetic phases were used as standards. The data were processed with the online ZAF-type correction. In addition, the ordered perthite grains are preferable for two-feldspar geothermometry, because the bulk composition of the disordered perthite grains may have been changed by a hydrothermal event (Benisek et al. 2004).

The weight percentages of plagioclase lamellae in perthite/mesoperthite were calculated from the areal/volume proportions of the lamellae estimated by computer image analysis of clear photomicrographs and/or backscattered electron images (Fig. 3), combined with the densities of the two feldspars [2.67 and 2.57 g/cm^3 for plagioclase and alkali feldspar, respectively; Smith (1974)]. This method was mainly based on the principles and procedures described in Hokada (2001). With the obtained weight percentages and the chemical compositions of both host and lamella, the re-integrated compositions of the pre-exsolution original alkali feldspar grains, and also the mole fraction of each component (Ab, An, Or) were computed (Tables 2 and 3).

If the two coexisting feldspars are in equilibrium, the activities (a_i) of Ab, An, and Or in the two phases are equal, T_{An}, T_{Ab}, and T_{Or}, determined using the formulas of two-feldspar geothermometers (e.g., Fuhrman and Lindsley 1988; Lindsley and Nekvasil 1989; Elkins and Grove 1990; Benisek et al. 2004, 2010), should be equal; however, they are rarely so, especially in high-grade metamorphic rocks. This problem is mainly caused by retrograde re-equilibration due to differential K-Na exchange (Kroll et al. 1993). Thus, some reintegration of the feldspar pairs is required to retrieve the compositions of the pairs at the peak metamorphic condition. We accomplished this reintegration using the Excel spreadsheet method of Benisek et al. (2004).

In Table 2, the analyzed compositions (C/Input) were from EMP analysis, and the calculated compositions [C(FL)/Output] were determined using the spreadsheet of Benisek et al. (2004). The calculated compositions represent the original compositions of the two feldspars when in equilibrium at the peak metamorphic condition. T(FL) (Table 2) represents the average of three similar temperatures (T_{An}, T_{Ab}, and T_{Or}) calculated at 8 kbar (see Guo et al. 2006, 2008; Santosh et al. 2009a) using the spreadsheet. Perthite/mesoperthite grains occur without associated plagioclase grains in the samples from Dongpo. The Ab, An, and Or contents of the perthite/mesoperthite were plotted on feldspar ternary diagrams (seeing Figs. 4 and 5), and the temperatures determined from the isotherms on which the compositions lie, were similar to the methods of Hokada (2001) and Santosh et al. (2007a).

The two-feldspar geothermometer for UHT metamorphism

Several models have been used to calculate temperatures using ternary feldspar data (Fuhrman and Lindsley 1988; Lindsley and Nekvasil 1989; Elkins and Grove 1990; Benisek et al. 2004). In this study, we have opted to use the model of Fuhrman and Lindsley (1988) as this method provides the best temperature estimates for UHT rocks for the following reasons. (1) Taking the Al-Si ordering of the Al-avoidance principle into account is better than treating the feldspar solution as an ideal single-site mixing, because the An contents in the plagioclase are 20–30%. Thus, the Al-avoidance models of Benisek et al. (2004) and Fuhrman and Lindsley (1988) are preferred. (2) Fuhrman and Lindsley (1988) refined the Seck (1971a, 1971b) experimental data by omitting the 650 °C experiments and adding higher temperature experiments. Lindsley and Nekvasil (1989) argued that the Fuhrman and Lindsley (1988) model was appropriate for high-temperature rocks, whereas Benisek et al. (2004) updated the formula by combining the experimental data of Seck (1971a, 1971b) with those of Elkins and Grove (1990). Their Al-avoidance model yielded similar temperatures as those of Fuhrman and Lindsley (1988). (3) Elkins and Grove (1990) calibrated the two-feldspar geothermometer using their own experimental data at 1–3 kbar, and compared with 1, 5, and 10 kbar of Seck (1971a, 1971b). The latter has been used in most two-feldspar geothermometers and is more appropriate for UHT metamorphic rocks that form at ~7–13 kbar (Harley 1998, 2008). Consequently, we prefer T(B) (Benisek et al. 2004) and T(FL) (Fuhrman and Lindsley 1988) for our samples, albeit only the temperatures from the Fuhrman and Lindsley (1988) model are listed in Tables 2 and 3.

Hokada (2001) also chose the Fuhrman and Lindsley (1988) model for estimating

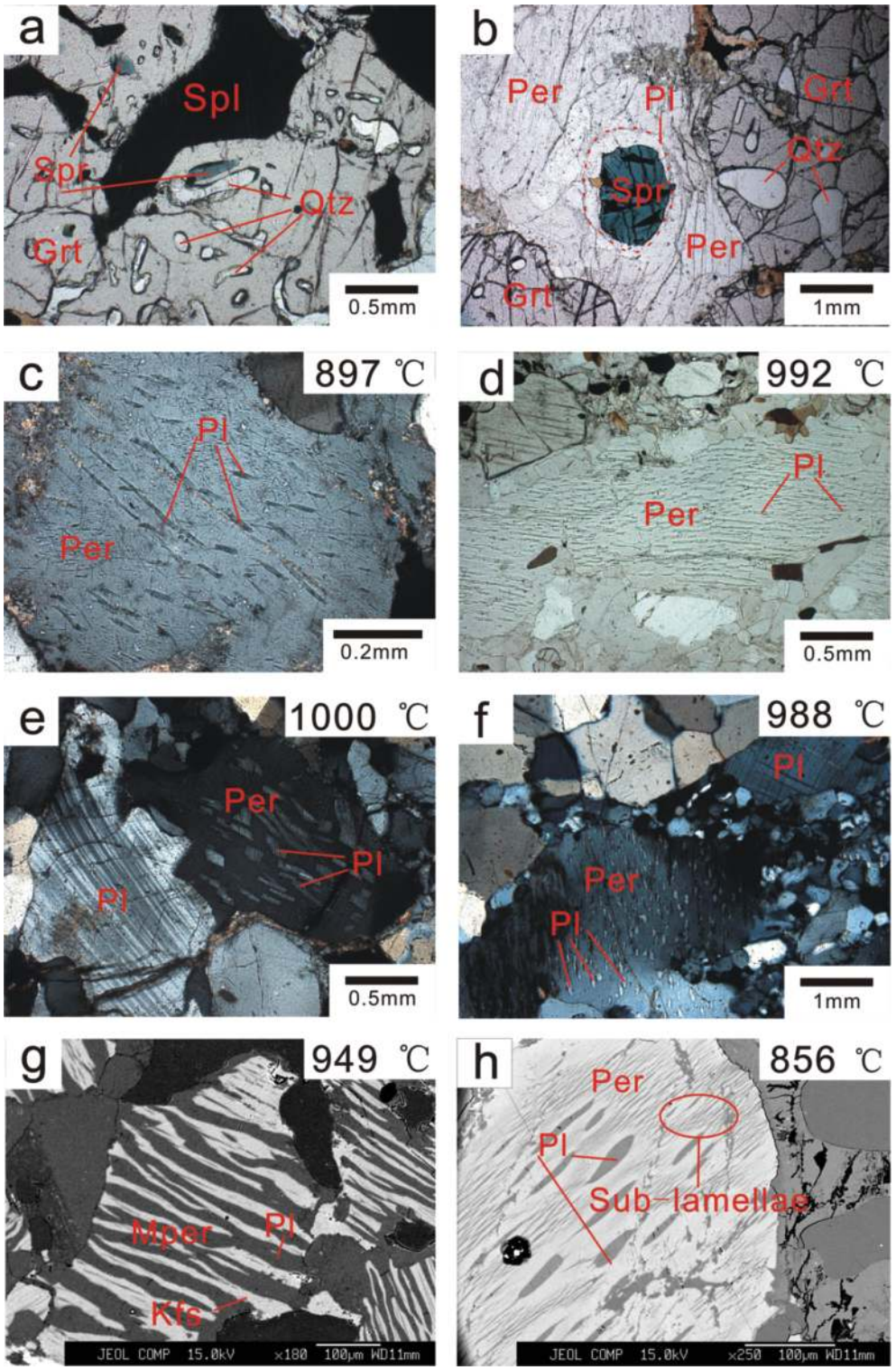

Figure 3. Photomicrographs and backscattered electron images of mineral assemblages in granulites from the Khondalite belt, North China craton. (**a**) Sapphirine, spinel, and quartz included in garnet from a Grt-Sil-Spr granulite (08dj12: locality 3 in Fig. 2b). (**b**) A large grain of sapphirine situated in matrix surrounded by plagioclase from a Grt-Sil-Spr granulite (08dj12: locality 3 in Fig. 2b). (**c**) Perthite with string lamellae from a Grt-Sil granulite (08tgs09-2: locality 2 in Fig. 2b). (**d**) Perthite with thick string plagioclase lamellae from a Grt-Sil-Bt-Pl granulite (08xwj01-1a: locality 4 in Fig. 2b). (**e**) Paired perthite and plagioclase from a Grt-Sil-Spr granulite (08dj03-5: locality 3 in Fig. 2b). (**f**) Paired perthite and plagioclase from a Grt-Sil-Bt-Pl granulite (08xwj03-3b: locality 4 in Fig. 2b). (**g**) Mesoperthite from a quartzo-feldspathic granulite (05dp02: locality 1 in Fig. 2a). (**h**) Perthite with clear sub-lamellae from a quartzo-feldspathic-garnet granulite (06dp20: locality 1 in Fig. 2a). The labeled temperatures were determined using the model of Fuhrman and Lindsley (1988).

TABLE 2. Analyzed and calculated compositions of feldspar pairs and estimated temperature results of the samples from the Dajing/Tuguiwula, Tuguishan, and Xuwujia outcrops

Sample	C/Input			C(FL)/Output			*T*(FL)
	Ab	Or	An	Ab	Or	An	°C
Tuguishan							
07tgs01-2	0.641	0.013	0.346	0.517	0.137	0.346	935
	0.236	0.702	0.062	0.262	0.676	0.062	
07tgs01-8	0.636	0.015	0.349	0.554	0.097	0.349	850
	0.2	0.762	0.038	0.227	0.735	0.038	
07tgs01-9	0.643	0.013	0.345	0.495	0.161	0.345	979
	0.252	0.668	0.08	0.279	0.641	0.080	
07tgs01-10	0.642	0.01	0.348	0.511	0.141	0.348	943
	0.231	0.704	0.065	0.264	0.671	0.065	
07tgs01-11	0.645	0.004	0.351	0.547	0.102	0.351	863
	0.202	0.757	0.041	0.232	0.727	0.041	
08tgs05-2	0.702	0.007	0.29	0.572	0.137	0.290	927
	0.313	0.624	0.063	0.313	0.624	0.063	
08tgs05-3	0.673	0.01	0.317	0.566	0.117	0.317	881
	0.253	0.702	0.045	0.258	0.697	0.045	
08tgs05-4	0.682	0.008	0.31	0.591	0.099	0.310	844
	0.248	0.716	0.036	0.248	0.716	0.036	
08tgs08a1-4	0.633	0.015	0.353	0.551	0.097	0.353	854
	0.181	0.78	0.039	0.228	0.733	0.039	
08tgs09-1	0.629	0.008	0.363	0.448	0.189	0.363	1037
	0.288	0.601	0.111	0.288	0.601	0.111	
08tgs09-2	0.629	0.013	0.359	0.530	0.112	0.359	892
	0.227	0.724	0.049	0.240	0.711	0.049	
08tgs11-4	0.622	0.011	0.367	0.523	0.110	0.367	889
	0.225	0.727	0.048	0.234	0.718	0.048	
08tgs11-6	0.62	0.01	0.37	0.522	0.108	0.370	885
	0.223	0.73	0.047	0.231	0.722	0.047	
08tgs12-1	0.63	0.008	0.361	0.535	0.103	0.361	868
	0.195	0.761	0.043	0.230	0.726	0.043	
08tgs12-2	0.623	0.01	0.367	0.529	0.104	0.367	873
	0.204	0.754	0.043	0.227	0.731	0.043	
08tgs18-1	0.645	0.012	0.342	0.526	0.131	0.342	918
	0.252	0.692	0.056	0.257	0.687	0.056	
08tgs18-3	0.642	0.012	0.346	0.544	0.110	0.346	900
	0.264	0.682	0.054	0.264	0.682	0.054	
08tgs19-1	0.647	0.008	0.345	0.532	0.123	0.345	908
	0.245	0.702	0.053	0.253	0.694	0.053	
08tgs19-2	0.633	0.011	0.356	0.503	0.141	0.356	963
	0.28	0.641	0.078	0.280	0.641	0.078	
Dajing/Tuguiwula							
08dj03-2	0.645	0.009	0.346	0.518	0.136	0.346	932
	0.233	0.706	0.061	0.261	0.678	0.061	
08dj03-4	0.649	0.013	0.338	0.486	0.176	0.338	996
	0.277	0.636	0.087	0.287	0.626	0.087	
08dj03-5	0.651	0.007	0.342	0.486	0.172	0.342	993
	0.266	0.645	0.088	0.287	0.624	0.088	
08dj03-6	0.647	0.012	0.341	0.498	0.161	0.341	973
	0.262	0.664	0.075	0.276	0.650	0.075	
08dj03-7	0.634	0.016	0.35	0.535	0.115	0.350	905
	0.257	0.689	0.054	0.257	0.689	0.054	
08dj03-8	0.648	0.013	0.339	0.513	0.148	0.339	952
	0.272	0.66	0.068	0.272	0.660	0.068	
08dj03-9	0.65	0.008	0.341	0.527	0.131	0.341	919
	0.255	0.691	0.055	0.256	0.690	0.055	
08dj05-1	0.654	0.009	0.337	0.504	0.159	0.337	991
	0.307	0.6	0.093	0.307	0.600	0.093	
08dj05-2	0.653	0.01	0.338	0.532	0.131	0.338	920
	0.257	0.688	0.056	0.261	0.684	0.056	
08dj05-5	0.641	0.011	0.347	0.512	0.140	0.347	946
	0.27	0.663	0.067	0.270	0.663	0.067	
08dj05-6	0.646	0.009	0.345	0.503	0.152	0.345	998
	0.322	0.574	0.105	0.322	0.574	0.105	
08dj09-1	0.651	0.009	0.34	0.555	0.105	0.340	891
	0.268	0.68	0.052	0.268	0.680	0.052	
08dj11-3	0.637	0.014	0.349	0.561	0.090	0.349	832
	0.183	0.783	0.034	0.220	0.746	0.034	
08dj12b-1	0.653	0.009	0.339	0.499	0.163	0.339	979
	0.278	0.642	0.08	0.283	0.637	0.080	
08dj12b-2	0.648	0.009	0.343	0.510	0.147	0.343	950
	0.242	0.693	0.066	0.267	0.668	0.066	
08dj13-4	0.663	0.011	0.326	0.556	0.118	0.326	924
	0.303	0.628	0.068	0.303	0.628	0.068	
Xuwujia							
08xwj01-1a	0.749	0.009	0.242	0.539	0.219	0.242	997
	0.362	0.547	0.091	0.363	0.546	0.091	
08xwj03-2	0.691	0.012	0.297	0.533	0.170	0.297	966
	0.293	0.633	0.074	0.306	0.620	0.074	
08xwj03-3a	0.691	0.011	0.298	0.493	0.209	0.298	1019
	0.316	0.583	0.101	0.322	0.577	0.101	
08xwj03-3b	0.69	0.016	0.294	0.510	0.196	0.294	1003
	0.323	0.586	0.092	0.323	0.586	0.092	
08xwj04a-3	0.679	0.011	0.31	0.515	0.175	0.310	980
	0.239	0.681	0.08	0.301	0.619	0.080	
08xwj04b-2	0.709	0.012	0.28	0.523	0.198	0.280	1000
	0.335	0.567	0.097	0.342	0.560	0.097	

Note: The first row is Pl and the second is Afs.

the UHT conditions of the Archean Napier Complex, East Antarctica. Their reasoning was based on the assumption that the inter-crystalline coupled CaAl-(Na,K)Si exchange was slow and ceased immediately after the peak metamorphic condition, whereas the simple K-Na exchange was easier and continued to a lower temperature. Therefore, the K component in plagioclase would diffuse away from the crystal before the exsolution lamellae precipitated, and the re-integrated compositions of antiperthite in the same thin section with perthite or mesoperthite should yield lower temperatures. The occurrence of lamellae-free plagioclase provides strong confirmation of this model, as seen in Figures 2a and 2c of Hokada (2001). Our results also demonstrate that the lamellae-free plagioclase grains yield lower temperatures than the coexisting perthite grains (Figs. 4 and 5a). The Fuhrman and Lindsley (1988) model yielded a lower temperature for antiperthite than perthite and mesoperthite, whereas the models of Lindsley and Nekvasil (1989) and Elkins and Grove (1990) yielded exactly the opposite results. Therefore, Hokada (2001) preferred temperature calculations based on the Fuhrman and Lindsley (1988) model. Moreover, Štípská and Powell (2005) chose the Fuhrman and Lindsley (1988) model, as suggested by Hokada (2001) for their high-temperature rocks (1000–1100 °C at 8 kbar).

Benisek et al. (2010) recently presented a mixing model for high structural state ternary feldspars based exclusively on calorimetric and volumetric measurements, which is distinctly different from the model used herein. To be cautious, we also applied this model to our data. However, the calculated temperatures in the range of 400–500 °C are unreasonable, compared to 900–1000 °C of *T*(FL) using the Excel spreadsheet of Benisek et al. (2004). The reason is unknown. Furthermore, the results from the Dongpo outcrop, based on the model of Benisek et al. (2010), show that the mesoperthite and perthite within the same thin section (sample 05dp02) almost lie on the same isotherm (Fig. 5a). The data also demonstrate that the perthite yields a temperature even higher than mesoperthite, as do the samples from the Xuwujia outcrop (Fig. 5b), which conflict with our conventional views. Thus, the new model of Benisek et al. (2010) is unsuitable for our samples.

The precision of the calculated temperatures

The precision of the calculated temperatures is mainly affected by the uncertainty of the detected feldspar compositions and the Margules parameters of the mixing models. The perthite and mesoperthite of our samples do not represent obvious exsolved core and non-exsolved rim, and the compositions of the host and lamellae are homogeneous without compositional zoning preserved. We did not calculate the uncertainty in this work. Benisek et al. (2004) estimated the uncertainties of the calculated temperatures according to Gaussian distributions with standard deviations as assumed, by generating mole fractions that scattered around the perthite and antiperthite within appropriate compositional standard errors, and obtained a mean and standard deviation of 915 ± 19 °C. We estimate that the uncertainty of the calculated temperatures from our chemical analyses may be <20 °C.

The Margules parameters of the mixing models are mainly based on the phase-equilibrium experimental data of Seck (1971a, 1971b) and Elkins and Grove (1990), whose data were generated at relatively low pressures and temperatures, over a small range. Thus these authors had to rely on a substantial extrapolation of thermodynamic equations to yield some missing Margules parameters. Moreover, they all ignored the structural transition in plagioclase, rendering the use of their equations for extrapolation problematic. In addition, the phase-equilibria experi-

TABLE 3. Analyzed chemical compositions, re-integrated original compositions of feldspars and estimated temperatures of samples from the Dongpo outcrop

Sample	Feldspar	SiO_2	TiO_2	Al_2O_3	Cr_2O_3	FeO	MnO	MgO	CaO	BaO	NiO	Na_2O	K_2O	Total	Ab	Or	An	Cls	*T*(FL)
06dp20-3	Pl(in per)	62.98	0.08	23.09	0.05	0.06	0.03	0.01	4.38	0	0.04	9.17	0.12	100	78.61	0.65	20.74	0	
	Per	63.73	0.01	18.63	0	0	0	0.02	0.12	0.65	0.02	1.52	14.38	99.09	13.6	84.71	0.59	1.1	
	Afs	63.63	0.02	19.25	0.01	0.01	0	0.02	0.72	0.56	0.02	2.59	12.38	99.21	23.05	72.49	3.52	0.94	830
04dq1-3-2	Pl(in per)	58.62	0.03	25.69	0.02	0.01	0.03	0.01	7.41	0	0.01	7.2	0.12	99.15	63.32	0.68	35.99	0	
	Per	64.2	0.05	18.88	0.01	0.02	0	0.03	0.28	0.36	0.01	1.54	14.37	99.75	13.76	84.25	1.39	0.6	
	Afs	63.86	0.05	19.29	0.01	0.02	0	0.03	0.71	0.34	0.01	1.88	13.51	99.71	16.77	79.17	3.5	0.57	819
04dq1-3-3	Pl(in per)	58.17	0	26.3	0.01	0.06	0	0	7.72	0	0.03	6.98	0.18	99.44	61.41	1.05	37.54	0	
	Per	64.44	0.01	18.92	0.06	0.03	0	0	0.23	0.5	0	1.5	14.26	99.95	13.47	84.52	1.16	0.85	
	Afs	64	0.01	19.44	0.05	0.03	0	0	0.76	0.47	0	1.88	13.27	99.91	16.9	78.55	3.76	0.79	844
05dp04-1	Pl(in per)	63.82	0.05	23.51	0.2	0.03	0	0.01	3.89	0.1	0.01	8.59	0.6	100.8	77.02	3.54	19.26	0.17	
	Per	65.31	0.08	18.35	0.05	0.02	0	0	0.53	0.4	0	1.7	14.14	100.58	14.91	81.87	2.56	0.66	
	Afs	65.19	0.08	18.77	0.06	0.02	0	0	0.79	0.38	0	2.25	13.06	100.6	19.79	75.71	3.87	0.62	837
05dp04-2	Pl(in per)	62.59	0.04	23.65	0	0	0.01	0	5.18	0	0	8.93	0.16	100.56	75.03	0.91	24.06	0	
	Per	65.98	0.08	18.04	0	0.03	0	0.01	0.25	0.44	0.07	3.2	12.13	100.24	28.05	69.99	1.23	0.73	
	Afs	65.5	0.07	18.83	0	0.02	0	0.01	0.94	0.38	0.06	4	10.45	100.28	34.88	59.96	4.54	0.62	884
05dp02-1	Pl(in mper)	65.49	0	21.24	0.01	0.01	0	0	3.34	0	0	10.34	0.2	100.63	83.94	1.08	14.98	0	
	Mper	65.97	0.06	17.96	0	0	0.02	0.02	0.05	0.45	0.05	1.01	15.81	101.38	8.75	90.31	0.22	0.72	
	Afs	65.74	0.03	19.5	0	0.01	0.01	0.01	1.59	0.24	0.02	5.39	8.47	101.03	45.36	46.87	7.4	0.37	946
05dp02-2	Pl(in per)	65.67	0.05	21.47	0.03	0.03	0.02	0	3.31	0.01	0	10.36	0.07	101	84.67	0.39	14.93	0.01	
	Per	65.69	0.04	17.96	0.03	0	0	0.01	0.06	0.39	0.04	1	15.32	100.55	8.97	90.1	0.28	0.65	
	Afs	65.68	0.04	18.94	0.03	0.01	0	0.01	0.97	0.28	0.03	3.62	11.05	100.68	31.55	63.34	4.65	0.46	890
05dp02-3	Pl(in mper)	65.76	0.01	21.42	0	0.04	0	0	3.35	0	0	10.18	0.16	100.91	83.9	0.85	15.26	0	
	Mper	65.44	0	17.82	0	0.05	0.03	0.01	0.01	0.43	0.05	0.97	15.42	100.23	8.69	90.54	0.05	0.72	
	Afs	65.62	0	19.8	0	0.04	0.01	0.01	1.85	0.19	0.02	6.04	7.02	100.6	51.53	39.45	8.71	0.31	952
05dp02-4	Pl(in mper)	66.28	0	21.27	0.13	0.06	0	0.02	3.02	0	0.03	10.38	0.12	101.31	85.56	0.67	13.77	0	
	Mper	66.08	0.02	17.79	0.04	0.02	0	0.02	0.05	0.34	0	1.21	15.54	101.09	10.48	88.73	0.24	0.55	
	Afs	65.52	0.01	19.42	0.08	0.04	0	0.02	1.59	0.16	0.02	5.96	7.37	100.2	50.87	41.35	7.52	0.25	938

Note: Temperature (°C) derived from the isotherm on which the feldspar was plotted.

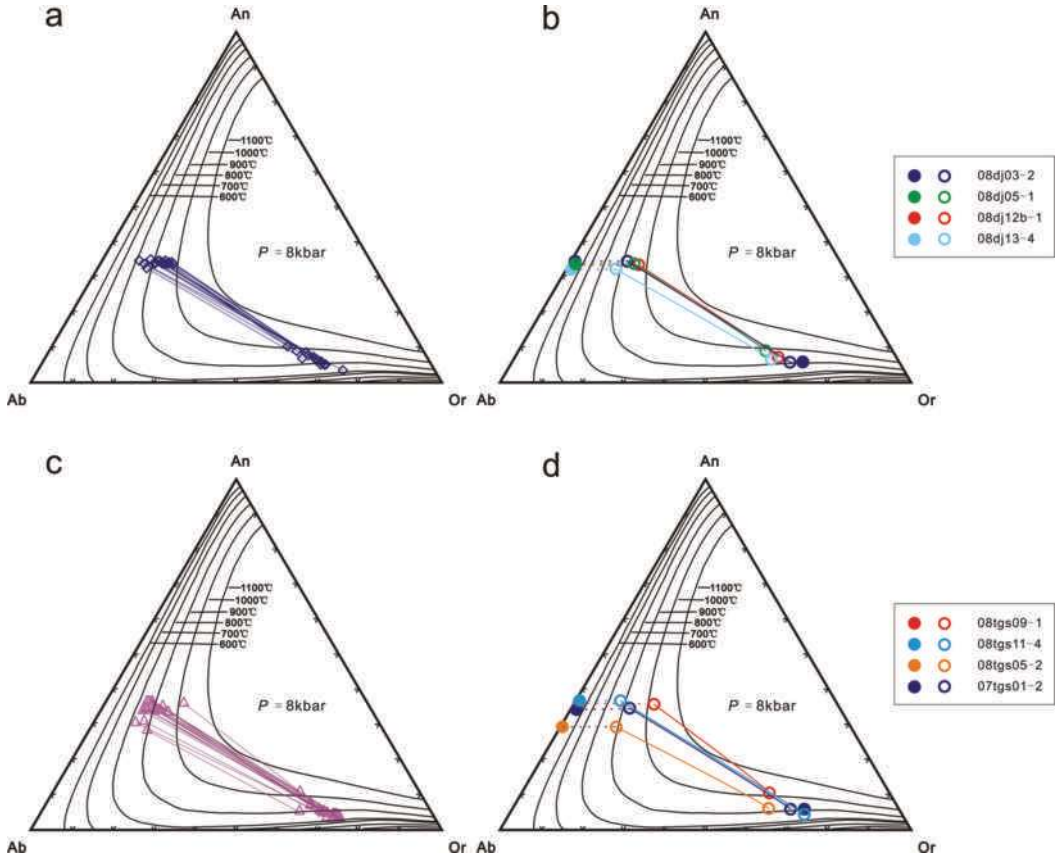

FIGURE 4. (**a**) Calculated compositions (open symbols) of perthite-plagioclase pairs of Grt-Sil-Spr granulites from the Dajing/Tuguiwula area. (**b**) Selected analyzed (closed symbols) and calculated compositions (open symbols) of perthite-plagioclase pairs of Grt-Sil-Spr granulites from **a**. (**c**) Calculated compositions (open symbols) of perthite-plagioclase pairs of Grt-Sil granulite from the Tuguishan area. (**d**) Selected analyzed (closed symbols) and calculated compositions (open symbols) of perthite-plagioclase pairs from **c**. Isotherms are determined using the model of Fuhrman and Lindsley (1988) at 8 kbar. See text for details.

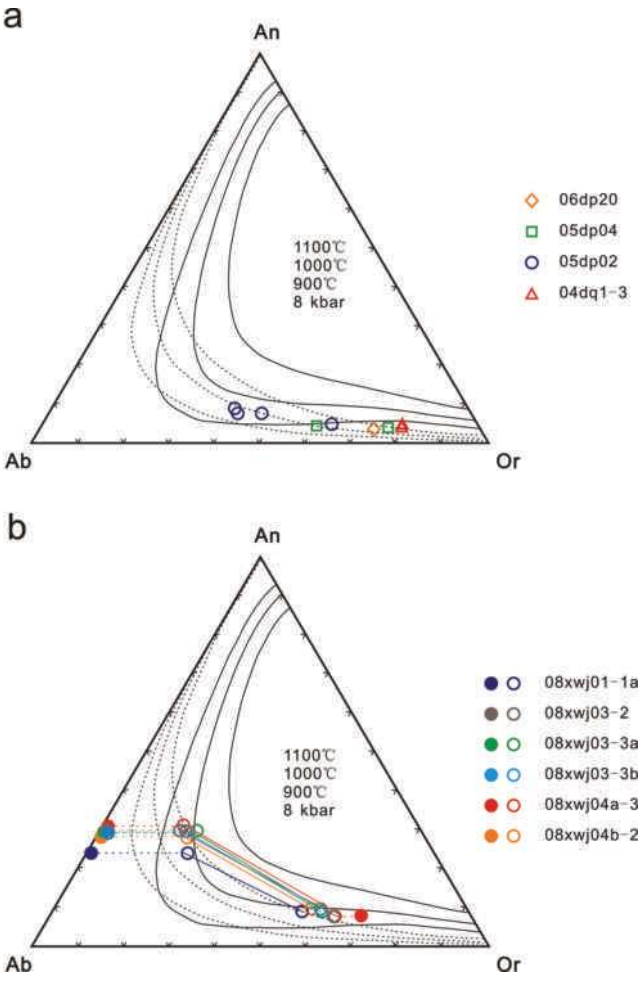

FIGURE 5. (**a**) Ternary feldspar diagram showing the compositions of the perthite grains and mesoperthite grains from the Dongpo area. (**b**) Analyzed (closed symbols) and calculated compositions (open symbols) of perthite-plagioclase pairs of Grt-Sil-Bt-Pl granulites from the Xuwujia area. Isotherms are based on the Fuhrman and Lindsley (1988) model (solid line) and the Benisek et al. (2010) model (dashed line) at 8 kbar. See text for details.

ments between 600 and 900 °C do not guarantee the achievement of equilibrium (Štípská and Powell 2005; Benisek et al. 2010). A satisfactory model is needed that involves additional higher pressure and temperature experiments. Nevertheless, the *T*(B) and *T*(FL) models appear to be the most appropriate for high-grade metamorphic rocks among the existent models.

We calculated the temperatures under different pressure conditions and found that pressure had a relatively small influence on temperature of <5 °C/kbar. Our calculations also suggest that the pressure shows a positive relationship with temperature according to the Benisek et al. (2004) model, but a negative relationship according to the Fuhrman and Lindsley (1988) model. In any case, the role of pressure seems to have only a negligible influence on the calculated temperatures.

Raase (1998) showed that the BaO content in feldspar pairs might slightly affect the estimated temperature. The BaO content of the feldspars was not analyzed in our electron microprobe analyses. Based on previous chemical data from the same outcrops with BaO determinations (unpublished data), the plagioclase lamellae in perthite from these rocks contain <0.5% celsian (Cls), and the re-integrated pethites have <1% celsian. In the case of 1% celsian component in a perthite, only 1 °C fluctuation is generated. Therefore, the celsian content in feldspar pairs was disregarded for the temperature estimations.

We considered the influence of many sub-lamellae in perthite grains (Fig. 3h), which were too small to be analyzed separately from the host by the electron microprobe (<3 μm in general). However, we selected perthite grains with a homogeneous host in our study to avoid these effects. Also, it is better in principle to take into account the three-dimensional geometry of exsolution features and the densities of the host and lamellae that will influence the reintegration procedures to obtain the pre-exsolution compositions of perthite (Hokada 2001; Štípská and Powell 2005; Harley 2008).

RESULTS

The Grt-Sil-Spr granulites at the Dajing/Tuguiwula outcrop yield relatively high temperatures in the range of 832–998 °C (Table 2). Among the 16 analyzed pairs of feldspars, 14 pairs yield temperature in excess of 900 °C. In the ternary feldspar diagram (Fig. 4a), most tie-lines between the 16 feldspar pairs are parallel, suggesting that the feldspar pairs are in equilibrium. As shown in Figure 4b, where both the analyzed and calculated compositions of 4 feldspar pairs (samples 08dj03-2, 08dj05-1, 08dj12b-1, and 08dj13-4) selected from Figure 4a are plotted, the plagioclase grains sit on a lower isotherm than the perthite grains, and shift much more than the perthite grains (the distance between the analyzed and calculated compositions), which is ascribed to their small proportions compared with perthite. This may be caused by the relatively higher Or contents in the plagioclase host, compared with the An contents of the perthite. In the KFMASH *P-T* grid (Fig. 6a), the *P-T* paths of Santosh et al. (2007a, 2009a) are shown. The qualitative Santosh et al. (2007a) path plots at a higher pressure and is mainly based on the diagnostic mineral assemblages such as Spr+Qz and Opx+Sil+Qz. The quantitative Santosh et al. (2009a) path is based on a pseudosection calculation. The *P-T* estimates from the previous thermobarometry calculations are also shown (Santosh et al. 2007a). The temperatures obtained from the present study plot in the fields of Opx+Crd+Kfs+Qz and Opx+Sil+Qz.

Of the four samples from the Dongpo outcrop, the nine perthite grains analyzed (Table 3; Fig. 5a) yield temperatures of 819–952 °C. Four mesoperthite grains from a quartzo-feldspathic granulite (sample 05dp02) give the highest temperature estimates of 890–952 °C. The results from the Tuguishan, Dajing/Tuguiwula, and Xuwujia outcrops suggest that perthite compositions generally show very little or no shift (Figs. 4 and 5), ensuring that the temperatures computed from perthite without coexisting plagioclase are reliable. As shown in Figure 6a, the estimated temperatures of the Dongpo outcrop are much lower than those of Dajing/Tuguiwula, and are mainly in the fields of Bt+Grt+Qz and Opx+Crd+Kfs+Qz. However, the >900 °C temperature results are consistent with the *P-T* estimates of Guo et al. (2006, 2008).

The calculated temperatures of the Grt-Sil granulites from the Tuguishan outcrop are 844–1037 °C (Table 2). Sample 08tgs09-1 yields the highest temperature (1037 °C) with eight other pairs in excess of 900 °C. In the ternary feldspar diagram (Fig. 4c), most of the tie-lines between the 19 feldspar pairs are parallel. The analyzed and calculated compositions of four pairs (samples 07tgs01-2, 08tgs05-2, 08tgs09-1, and 08tgs11-4) selected from Figure 4c are plotted in Figure 4d, which shows that plagioclase compositions usually shift much more than perthite unlike the samples from the Dajing/Tuguiwula area. In the KFMASH *P-T* grid (Fig. 6b), the temperature results mainly plot in the Bt+Grt+Qz and Opx+Crd+Kfs+Qz fields, and even extend to the Spr+Qz field.

The samples from the Xuwujia outcrop yield very high temperatures (966–1019 °C) (Table 2), all in excess of 900 °C. Figure

5b shows the analyzed and calculated compositions of all feldspar pairs. The tie-lines are mutually parallel, and the chemical shifts of plagioclase from the Xuwujia outcrop are much larger than the plagioclase from the Tuguishan and Dajing/Tuguiwula outcrops. This accords with the small quantity of plagioclase in the Xuwujia samples. As shown in Figure 6b, these temperatures plot in the fields of Opx+Sil+Qz and Spr+Qz.

Discussion

The feldspars in our samples (i.e., paragneisses or metasedimentary rocks; Lu et al. 1992, 1996) all coexist with metamorphic minerals such as sillimanite, cordierite, or sapphirine in the matrix, minerals that obviously represent the mineral assemblages of the peak metamorphic condition. Detrital zircon cores from the studied rocks are mostly anhedral and spherical, and are interpreted to be a result of erosion during sedimentary transport (e.g., Wan et al. 2006; Xia et al. 2006, 2008; Santosh et al. 2007b, 2009b). There is no doubt that the studied feldspars are metamorphic phases, instead of survivors from original high-temperature crystallization of igneous protoliths, as mentioned by Štípská and Powell (2005), who doubted if ternary feldspars in high-grade metaigneous rocks could constrain conditions of metamorphism. Our calculated temperatures indeed represent the metamorphism conditions.

From Tables 2–3 and Figures 4–5, it is evident that the calculated temperatures vary over a wide range (~819–1037 °C), even within same thin section. These temperatures should be the closure temperatures for Al-Si intercrystalline exchange

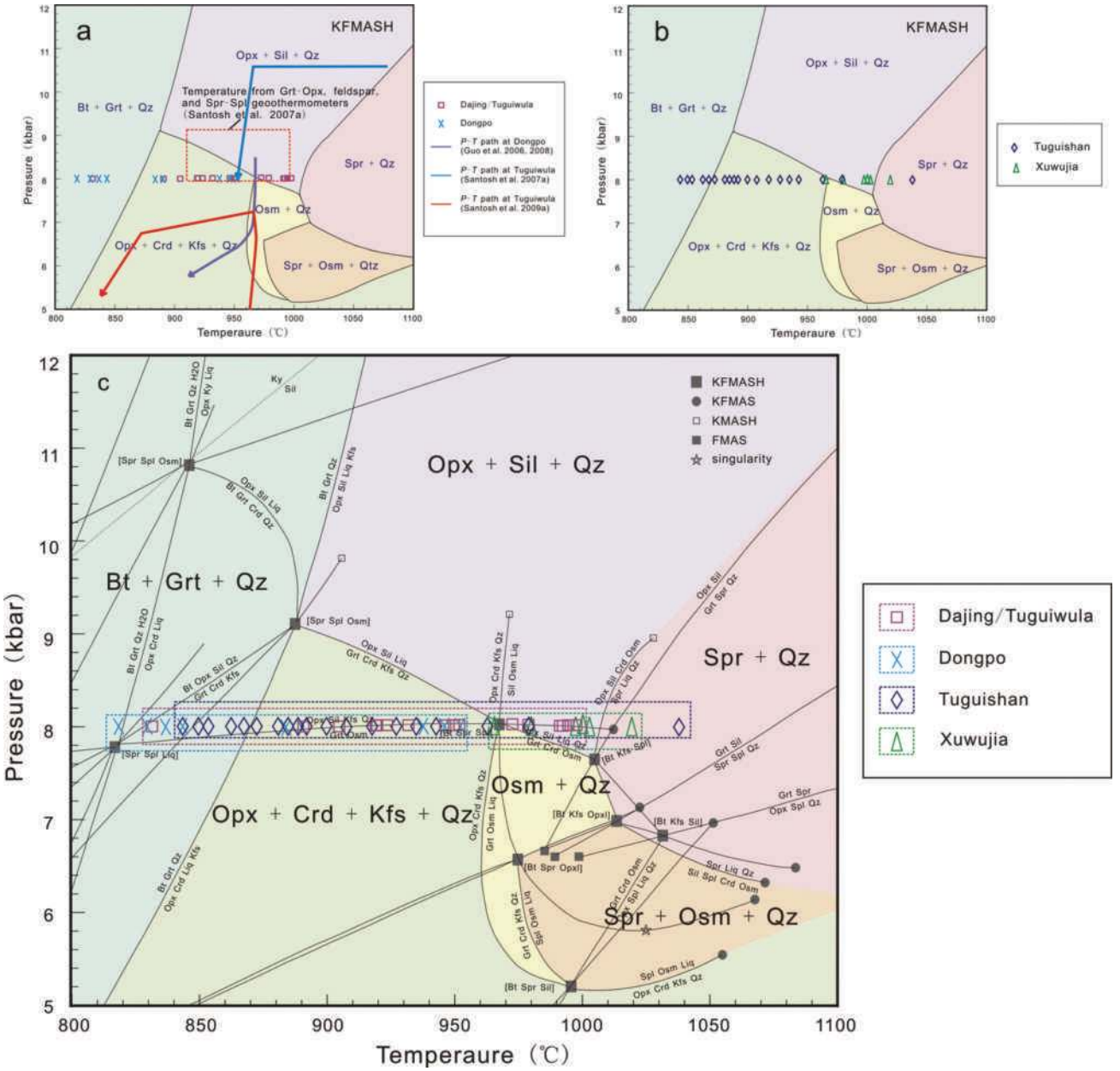

Figure 6. (**a**) Calculated metamorphic temperatures of the Dajing/Tuguiwula and Dongpo areas. The *P-T* paths of Santosh et al. (2007a, 2009a) are also shown. (**b**) Calculated metamorphic temperatures of the Tuguishan and Xuwujia areas. (**c**) All calculated metamorphic temperatures of the Khondalite belt, North China craton. The KFMASH *P-T* grid is modified after Kelsey et al. (2004).

in the feldspar pairs, which approximately correspond to peak metamorphic temperatures, because the intercrystalline CaAl-(Na,K)Si exchange is slow and ceases immediately after the peak metamorphic condition. For the samples from the Dongpo outcrop, the isotherms defined by the perthite analyses are minimum temperatures, which are even lower than the Al-Si closure temperatures. Therefore, all the calculated temperatures are minimum peak metamorphic temperatures, and not post-peak re-equilibration temperatures [see a comparison between coarse string perthite and the low-temperature products of recrystallization, in Fig. 2b of Raase (1998)]. Most of the perthite grains examined in this study were regular, coarse and continuous (Fig. 3), which were interpreted as evidence for slow cooling after regional metamorphism (Hayob et al. 1989). The perthite grains always yield higher temperatures when compared to irregular perthite grains, which may have been affected by re-equilibration. Raase (1998) suggested that the preservation of primary feldspar compositions was due to fluid-absent conditions, coarse grain size, and the predominance of a single feldspar. Each of the above conditions accord with those in our study areas.

In Figure 6c, all calculated temperatures are plotted on the KFMASH *P-T* grid (Kelsey et al. 2004). The majority of the calculated temperatures are in excess of 900 °C. Samples from the Tuguishan and Dongpo areas yield slightly lower temperatures, whereas those from the Dajing/Tuguiwula and Xuwujia areas yield relatively higher temperatures. Noteworthy are those from the Xuwujia outcrop that give temperatures up to 1019 °C.

Santosh et al. (2007a) reported UHT metamorphic conditions from the Dajing/Tuguiwula outcrop based on diagnostic mineral assemblages such as Spr+Qz and Opx+Sil+Qz, suggesting $T >$ 1000 °C and $P >$ 10 kbar peak metamorphism. Conventional geothermobarometric estimates also confirmed the UHT and minor retrograde conditions (930–970 °C at $P >$ 10 kbar for Al in Opx; 930–990 °C for Grt-Opx; and 910–940 °C for Spr-Spl). Furthermore, the temperature results of 900–1000 °C (at 8 kbar) determined by Santosh et al. (2007a) using the Elkins and Grove (1990) model are similar to our results of 908–1152 °C [*T*(EG): at 8 kbar] (Fig. 6a). In a recent study, Liu et al. (2010) reported the application of the revised Ti-in-zircon geothermometer to the UHT granulites at the Dajing/Tuguiwula outcrop. The highest temperature of 941 °C obtained in their study suggested cooling to ~940 °C from peak UHT conditions. Another range of 745–870 °C indicated zircon growth or recrystallization under lower temperatures. Our results from the Dajing/Tuguiwula outcrop are in agreement with the above results, and further confirm the UHT event in the Dajing/Tuguiwula outcrop. Moreover, the metamorphic temperatures estimated for samples from the Dongpo outcrop are well consistent with the 910–980 °C and 8 kbar peak conditions calculated from the THERMOCALC pseudosection by Guo et al. (2006, 2008).

The large number of metamorphic temperature estimates >900 °C suggest that all four localities investigated in this study have experienced UHT metamorphism regardless of whether or not indicative/diagnostic UHT minerals and mineral assemblages exist. The metamorphic temperatures presented here are consistent with previously recognized UHT metamorphism in Dajing/Tuguiwula and Dongpo. Our results also suggest that the granulites in the localities Tuguishan and Xuwujia newly reported in this study also experienced UHT metamorphism. This study demonstrates that the two-feldspar geothermometer may be an important tool in recognizing UHT rocks that do not preserve diagnostic UHT mineral assemblages either because they have inappropriate bulk compositions and/or have undergone later retrogressive metamorphism. In the Khondalite belt of the North China craton, for example, many metamorphic complexes (e.g., Helanshan Complex in the westernmost segment of the belt) contain pelitic granulites with assemblages of Spl+Qz without Spr+Qz and Opx+Sil±Qz. Detailed studies have not yet revealed assemblages indicative of UHT metamorphism. However, the two-feldspar geothermometer may help to identify UHT conditions in these rocks.

Our results further imply that the Paleoproterozoic UHT metamorphism may be more widespread within the Khondalite belt of North China craton than previously recognized. The finding of the new UHT metamorphic outcrops should stimulate further investigations into UHT rocks especially using the modified two-feldspar geothermometer. A well-constrained areal extent of UHT rocks will be helpful to evaluate whether the UHT metamorphism is local or regional, and to further understand the tectonic evolution of the Khondalite belt in the North China craton.

Acknowledgments

We sincerely thank Guochun Zhao, M. Santosh, and an anonymous reviewer for their constructive comments that helped to improve the manuscript and *American Mineralogist* Associate Editor Virginia L. Peterson for detailed modifications and significant comments. We also thank Artur Benisek for offering the sub-program software of the two-feldspar geothermometer and giving much help on its use. Brian Windley and M. Santosh are thanked for improving the written English of the manuscript. We also thank Qian Mao and Yuguang Ma for their assistance with electron microprobe analyses, and Peng Peng and Fu Liu for their help in field work. Chunming Wu is thanked for the helpful discussion. This study was supported financially by research grant no. 40730315 from the NSFC in China.

References cited

Benisek, A., Kroll, H., and Cemië, L. (2004) New developments in two-feldspar thermometry. American Mineralogist, 89, 1496–1504.

Benisek, A., Dachs, E., and Kroll, H. (2010) A ternary feldspar-mixing model based on calorimetric data: development and application. Contributions to Mineralogy and Petrology, 160, 327–337, doi: 10.1007/s00410-009-0480-8.

Elkins, L.T. and Grove, T.L. (1990) Ternary feldspar experiments and thermodynamic models. American Mineralogist, 75, 544–559.

Fuhrman, M.L. and Lindsley, D.H. (1988) Ternary-feldspar modeling and thermometry. American Mineralogist, 73, 201–215.

Guo, J.H., Shi, X., Bian, A.G., Xu, R.H., Zhai, M.G., and Li, Y.G. (1999) Pb isotopic composition of feldspar and U-Pb age of zircon from early Proterozoic granite in Sanggan area, North China craton: Metamorphism, crustal melting and tectono-thermal event. Acta Petrologica Sinica, 15, 199–207 (in Chinese with English abstract).

Guo, J.H., Wang, S.S., Sang, H.Q., and Zhai, M.G. (2001) ^{40}Ar-^{39}Ar age spectra of garnet porphyroblast: Implications for metamorphic age of high-pressure granulite in the North China craton. Acta Petrologica Sinica, 17, 436–442 (in Chinese with English abstract).

Guo, J.H., Sun, M., Chen, F.K., and Zhai, M.G. (2005) Sm-Nd and SHRIMP U-Pb zircon geochronology of high-pressure granulites in the Sanggan area, North China Craton: Timing of Paleoproterozoic continental collision. Journal of Asian Earth Sciences, 24, 629–642.

Guo, J.H., Chen, Y., Peng, P., Liu. F., Chen, L., and Zhang, L.Q. (2006) Sapphirine granulite from Daqingshan area, Inner Modolia-1.85Ga ultrahigh temperature (UHT) metamorphism. In Proceedings of National Conference on Petrology and Geodynamics in China (Nanjing), 215–218.

Guo, J.H., Chen, Y., Peng, P., Windley, B., and Sun, M. (2008) Highly silica-undersaturated sapphirine granulites from the Daqingshan area, Western Block, North China Craton: Paleoproterozoic UHT metamorphism. In, W.J. Xiao, M.G. Zhai, X.H. Li, and F. Liu, Eds., Proceedings of International Conference on Gondwana Correlation and Connection, Gondwana 13 in China (Dali), 64–65.

Harley, S.L. (1998) On the occurrence and characterization of ultrahigh-temperature crustal metamorphism. Geological Society of London, Special Publication, 138, p. 81–107.

——— (2004) Extending our understanding of ultrahigh temperature crustal metamorphism. Journal of Mineralogical and Petrological Sciences, 99, 140–158.
——— (2008) Refining the P-T records of UHT crustal metamorphism. Journal of Metamorphic Geology, 26, 125–154.
Hayob, J.L., Essene, E.J., Ruiz, J., Ortega-Gutiérrez, F., and Aranda-Gómez, J.J. (1989) Young high-temperature granulites from the base of the crust in central Mexico. Nature, 342, 265–268.
Hokada, T. (2001) Feldspar thermometry in ultrahigh-temperature metamorphic rocks: Evidence of crustal metamorphism attaining ~1100 °C in the Archaean Napier Complex, East Antarctica. American Mineralogist, 86, 932–938.
Hokada, T. and Suzuki, S. (2006) Feldspar in felsic orthogneiss as indicator for UHT crustal processes. Journal of Mineralogical and Petrological Sciences, 101, 260–264.
Jin, W. (1989) Early Precambrian geological evolution and metamorphic study on the basement of the north margin of the North China platform. Ph.D. thesis, Changchun College of Geology, China (in Chinese).
Kelsey, D.E. (2008) On ultrahigh-temperature crustal metamorphism. Gondwana Research, 13, 1–29.
Kelsey, D.E., White, R.W., Holland, T.J.B., and Powell, R. (2004) Calculated phase equilibria in K_2O-FeO-MgO-Al_2O_3-SiO_2-H_2O for sapphirine-quartz-bearing mineral assemblages. Journal of Metamorphic Geology, 22, 559–578.
Kroll, H., Evangelakakis, C., and Voll, G. (1993) Two-feldspar geothermometry: A review and revision for slowly cooled rocks. Contributions to Mineralogy and Petrology, 114, 510–518.
Kröner, A., Wilde, S.A., Zhao, G.C., O'Brien, P.J., Sun, M., Liu, D.Y., Wan, Y.S., Liu, S.W., and Guo, J.H. (2006) Zircon geochronology and metamorphic evolution of mafic dykes in the Hengshan Complex of northern China: Evidence for late Palaeoproterozoic extension and subsequent high-pressure metamorphism in the North China Craton. Precambrian Research, 146, 45–67.
Lindsley, D.H. and Nekvasil, H. (1989) A ternary feldspar model for all reasons. EOS, 70, 506.
Liu, J.Z., Qiang, X.K., Liu, X.S., and Ouyang, Z.Y. (2000) Dynamics and genetic grids of sapphirine-bearing spinel gneiss in Daqing Mountain orogen zone, Inner Mongolia. Acta Petrologica Sinica, 16, 245–255 (in Chinese with English abstract).
Liu, S.J., Li, J.H., and Santosh, M. (2010) First application of the revised Ti-in-zircon geothermometer to Paleoproterozoic ultrahigh-temperature granulites to Tuguiwula, Inner Mongolia, North China Craton. Contributions to Mineralogy and Petrology, 159, 225–235.
Lu, L.Z., Jin, S.Q., Xu, X.C., and Liu, F.L. (1992) The genesis of early Precambrian khondalite series in southeastern inner Mongolia and its potential mineral resources. Jilin scientific and technical Publishing House, Changchun, 1–25 p (in Chinese with English abstract).
Lu, L.Z., Xu, X.C., and Liu, F.L. (1996) The Precambrian khondalite series of northern China. Changchun Publishing House, Changchun, 16–39 p. (in Chinese).
Lund, M.D., Piazolo, S., and Harley, S.L. (2006) Ultrahigh temperature deformation microstructures in felsic granulites of the Napier Complex, Antarctica. Tectonophysics, 427, 133–151.
Peng, P., Guo, J.H., Zhai, M.G., and Bleeker, W. (2010) Paleoproterozoic gabbronoritic and granitic magmatism in the northern margin of the North China craton: Evidence of crust-mantle interaction. Precambrian Research, in press, doi:10.1016/j.precamres.2010.08.015.
Pilugin, S.M., Fonarev, V.I., and Savko, K.A. (2009) Feldspar thermometry of ultrahigh-temperature (≥1000 °C) metapelites from the Voronezh crystalline massif (Kursk-Besedino Granulite Block). Doklady Earth Sciences, 425, 201–204.
Prakash, D., Arima, M., and Mohan, A. (2006) Ultrahigh-temperature metamorphism in the Palni Hills, South India: Insights from feldspar thermometry and phase equilibria. International Geology Review, 48, 619–638.
Raase, P. (1998) Feldspar thermometry: A valuable tool for deciphering the thermal history of granulite-facies rocks, as illustrated with metapelites from Sri Lanka. The Canadian Mineralogist, 36, 67–86.
Rogers, J.J.W. and Santosh, M. (2002) Configuration of Columbia, a Mesoproterozoic supercontinent. Gondwana Research, 5, 5–22.
——— (2009) Tectonics and surface effects of the supercontinent Columbia. Gondwana Research, 15, 373–380.
Santosh, M. (2010) Assembling North China Craton within the Columbia supercontinent: The role of double-sided subduction. Precambrian Research, 178, 149–167.
Santosh, M. and Kusky, T. (2010) Origin of paired high pressure–ultrahigh-temperature orogens: a ridge subduction and slab window model. Terra Nova, 22, 35–42.
Santosh, M., Sajeev, K., and Li, J.H. (2006) Extreme crustal metamorphism during Columbia supercontinent assembly: Evidence from North China Craton. Gondwana Research, 10, 256–266.
Santosh, M., Tsunogae, T., Li, J.H., and Liu, S.J. (2007a) Discovery of sapphirine-bearing Mg-Al granulites in the North China Craton: Implications for Paleoproterozoic ultrahigh temperature metamorphism. Gondwana Research, 11, 263–285.
Santosh, M., Wilde, S.A., and Li, J.H. (2007b) Timing of Paleoproterozoic ultrahigh-temperature metamorphism in the North China Craton: Evidence from SHRIMP U-Pb zircon geochronology. Precambrian Research, 159, 178–196.
Santosh, M., Sajeev, K., Li, J.H., Liu, S.J., and Itaya, T. (2009a) Counterclockwise exhumation of a hot orogen: The Paleoproterozoic ultrahigh-temperature granulites in the North China Craton. Lithos, 110, 142–152.
Santosh, M., Wan, Y.S., Liu, D.Y., Dong, C.Y., and Li, J.H. (2009b) Anatomy of zircons from an ultrahot orogen: The amalgamation of the North China Craton within the supercontinent Columbia. The Journal of Geology, 117, 429–443.
Santosh, M., Zhao, D.P., and Kusky, T. (2010) Mantle dynamics of the Paleoproterozoic North China Craton: A perspective based on seismic tomography. Journal of Geodynamics, 49, 39–53.
Seck, H.A. (1971a) Koexistierende alkalifeldspäte und plagioklase im system $NaAlSi_3O_8$-$KAlSi_3O_8$-$CaAl_2Si_2O_8$-H_2O bei temperaturen von 650 °C bis 900 °C. Neues Jahrbuch Mineralogie Abhandlungen, 115, 315–345.
Seck, H.A. (1971b) Der einfluss des drucks auf die zusammensetzung koexistierender alkalifeldspäte und plagioklase. Contributions to Mineralogy and Petrology, 31, 67–86.
Smith, J.V. (1974) Feldspar Minerals. Volume 1. Crystal structure and physical properties, 625 p. Springer-Verlag, Berlin.
Štípská, P. and Powell, R. (2005) Does ternary feldspar constrain the metamorphic conditions of high-grade meta-igneous rocks? Evidence from orthopyroxene granulites, Bohemian Massif. Journal of Metamorphic Geology, 23, 627–647.
Wan, Y.S., Song, B., Liu, D.Y., Wilde, S.A., Wu, J.S., Shi, Y.R., Yin, X.Y., and Zhou, H.Y. (2006) SHRIMP U-Pb zircon geochronology of Palaeoproterozoic metasedimentary rocks in the North China Craton: Evidence for a major Late Palaeoproterozoic tectonothermal event. Precambrian Research, 149, 249–271.
Wu, C.H., Li, H.M., Zhong, C.T., and Chen, Q.A. (1998) The ages of zircon and rutile (cooling) from khondalite in Huangtuyao, Inner Mongolia. Geological Review, 44, 618–626 (in Chinese with English abstract).
Xia, X.P., Sun, M., Zhao, G.C., and Luo, Y. (2006) LA-ICP-MS U-Pb geochronology of detrital zircons from the Jining Complex, North China Craton and its tectonic significance. Precambrian Research, 144, 199–212.
Xia, X.P., Sun, M., Zhao, G.C., Wu, F.Y., Xu, P., Zhang, J., and He, Y.H. (2008) Paleoproterozoic crustal growth in the Western Block of the North China Craton: Evidence from detrital zircon Hf and whole rock Sr-Nd isotopic compositions of the khondalites from the Jining Complex. American Journal of Science, 308, 304–327.
Yin, C.Q., Zhao, G.C., Sun, M., Xia, X.P., Wei, C.J., Zhou, X.W., and Leung, W.H. (2009) LA-ICP-MS U-Pb zircon ages of the Qianlishan Complex: Constrains on the evolution of the Khondalite Belt in the Western Block of the North China Craton. Precambrian Research, 174, 78–94.
Zhai, M.G., Guo, J.H., Li, Y.G., Liu, W.J., Peng, P., and Shi, X. (2003) Two linear granite belts in the central-western North China Craton and their implication for Late Neoarchaean-Palaeoproterozoic continental evolution. Precambrian Research, 127, 267–283.
Zhao, G.C., Wilde, S.A., Cawood, P. A., and Lu, L.Z. (1999) Tectonothermal history of the basement rocks in the western zone of the North China Craton and its tectonic implications. Tectonophysics, 310, 37–53.
Zhao, G.C., Wilde, S.A., Cawood, P.A., and Sun, M. (2001) Archean blocks and their boundaries in the North China Craton: lithological, geochemical, structural and P-T path constraints and tectonic evolution. Precambrian Research, 107, 45–73.
——— (2002) SHRIMP U-Pb zircon ages of the Fuping Complex: Implications for late Archean to Paleoproterozoic accretion and assembly of the North China Craton. American Journal of Science, 302, 191–226.
Zhao, G.C., Sun, M., Wilde, S.A., and Li, S.Z. (2005) Late Archean to Paleoproterozoic evolution of the North China Craton: Key issues revisited. Precambrian Research, 136, 177–202.
Zhao, G.C., Wilde, S.A., Sun, M., Li, S.Z., Li, X.P., and Zhang, J. (2008a) SHRIMP U–Pb zircon ages of granitoid rocks in the Lüliang Complex: Implications for the accretion and evolution of the Trans-North China Orogen. Precambrian Research, 160, 213–226.
Zhao, G.C., Wilde, S.A., Sun, M., Guo, J.H., Kröner, A., Li, S.Z., Li, X.P., and Zhang, J. (2008b) SHRIMP U-Pb zircon geochronology of the Huai'an complex: constrains on late Archean to Paleoproterozoic magmatic and metamorphic events in the Trans-North China Orogen. American Journal of Science, 308, 270–303.
Zhong, C.T., Deng, J.F., Wan, Y.S., Mao, D.B., and Li, H.M. (2007) Magma recording of Paleoproterozoic orogeny in central segment of northern margin of North China Craton: Geochemical characteristics and zircon SHRIMP dating of S-type granitoids. Geochimica, 36, 585–600.

Manuscript received January 14, 2010
Manuscript accepted September 19, 2010
Manuscript handled by Virginia Peterson